International Journal of Advanced Engineering Research and Science (IJAERS) *[Vol-6, Issue-1, Jan- 2019]*
https://dx.doi.org/10.22161/ijaers.6.1.17 *ISSN: 2349-6495(P) | 2456-1908(O)*

On the Joint Symbol and Channel Estimation for Three-Hop MIMO Relaying Links

Leandro R. Ximenes

School of Technology, State University of Campinas (UNICAMP), Limeira, Brazil
Email: leandro@ft.unicamp.br

***Abstract*—*There is a consensus that cooperative communication is a key technology for the upcoming generations of mobile communications. Whether under the Coordinated Multipoint (CoMP), Device-to-Device (D2D) communication or Internet of Things (IoT) scopes, there is little doubt that a more decentralized network, where several communicating agents smartly cooperate to improve data rate and reliability, is fundamental to cope with the always scarce resources of energy and bandwidth. When relaying stations are deployed to increase signal coverage and to provide cooperative diversity, the concatenation of two or more point-to-point MIMO channels impose a restriction on conventional algorithms for channel estimation. Although single-relay, two-hop Amplify-and-Forward (AF) systems have been reasonably investigated, there are enough evidences that more transmission hops will be a common scenario in the next years. This work proposes a semi-blind receiver for the task of joint symbol and channel estimation in a three-hop AF MIMO system. Resorting to a Nested PARAFAC tensor model, new estimating equations were derived, along studies on the uniqueness and identifiability conditions concerning the aforementioned receiver. Simulations corroborate the validity of the receiver as an effective option.*

Keywords*—*Amplify-and-Forward , Cooperative communications, Relaying, Tensor decomposition.

I. INTRODUCTION

In wireless communications, relay stations havebeen extensively deployed to increase the signal coverage in a broadcast transmission [15]. In recent years, relaying also has been used to provide digital receivers with what is called cooperative diversity, where a relay might work with single-antenna transmitters to emulate a virtual array of antennas. In this sense, the benefits of spatial transmit diversity could be obtained without a increase of the number of transmit antennas.

The simplest of the relaying protocols is called Amplify-and-Forward (AF) As its name suggests, the incoming signals are amplified, and then forwarded to the intended destination. The main advantage of this non-regenerative process is that no complex decodingis performed at the relay, so its hardware and software complexities arereduced with comparison to the so-called regenerative protocols, such as the Decode-and-Forward (DF), favoring its mass implementation [15-16]. As a drawback, due to its simple operation, noise and interference are also amplified, limiting the benefits of relaying.

Another disadvantage of the AF protocol is related to the task of channel estimation. Besides the usual need of the Channel State Information (CSI) for symbol detection, many system optimization techniques demand the knowledge of the various channels that compose a relaying network [1, 8-10]. The absence of a powerful processing unit at the relay leaves all this work to the destination node, which is usually inapt to dissociate the cascaded *source-relay* and *relay-destination* channels under conventional transmission protocols.

The issue of channel estimation in two-hop AF MIMO systems have been addressed in few state-of-the-art works [5-7,14] by using training sequences and by [11, 12] in a semi-blind fashion. However, when it comes to the multi-hop systems, with more than one serial relay in the communication link, there is usually a lack of related works. This is particularly concerning since the future of wireless communications points towards ever more decentralized networks, such as Device-to-Device (D2D) communications technologies, where longer chains of connected relaying devices can be expected. For a three-hop (two relays) link, [2] have resorted to the combination of PARAFAC and Tucker tensor models to estimate the channel. However, [2] resorts once again to the use of pilot symbols, disregarding the benefits of the joint estimation of symbols and channels.In [18] the authors generalized the works of [11,12] for any number of hops.

This work proposes a three-hop AF MIMO system, where both relays and the source node applies a Khatri-Rao Space-Time (KRST) coding over the signals prior to their transmission. In this way, the receiver can arrange the signals into a 5^{th}-order tensor following a Nested PARAFAC model, from which the three-hop

https://dx.doi.org/10.22161/ijaers.6.1.17 *ISSN: 2349-6495(P) | 2456-1908(O)*

channels and symbols can be estimated by a closed-form algorithm. Notably, this proposed tensor model is an expansion of the 4^{th}-order model ,holding similar properties/advantages. Studies on the uniqueness of the proposed model and and on identifiability conditions for the proposed receiver are also carried out, along the presentation of its computational complexity and performance in terms of Bit Error Rate (BER) and channel Normalized Mean Square Error (NMSE).

The main contributions are:

1. Derivation of new unfolded equations for the three-hop system, for both signals and noise terms;
2. Proposal of a theorem on the essential uniqueness of the system model;
3. Discussion on the computational complexity and on the achievable spectral efficiency of the proposed method.

1.1 Notations and fundamentals of tensors

Scalars, column vectors, matrices, and tensors are denoted by lower-case (x), boldface lower-case $(\mathbf{x})$, boldface capital $(\mathbf{X})$, and calligraphic $(\mathcal{X})$ letters, respectively. $\mathbf{X}^T$, $\mathbf{X}^*$, $\mathbf{X}^\dagger$, $\mathbf{X}_{l.}$ and $\mathbf{X}_{.m}$ are the transpose, the conjugate, the pseudoinverse, the l^{th} row, and the m^{th} column of $\mathbf{X} \in \mathbb{C}^{L\times M}$, respectively. $D_n(\mathbf{X})$ stands for the diagonal matrix formed from the elements of $\mathbf{X}_{n.}$. Given a third-order tensor $\mathcal{X} \in \mathbb{C}^{I\times J\times K}$, with entry $x_{i,j,k}$, the matrices $\mathbf{X}_{JK\times I}$, $\mathbf{X}_{KI\times J}$ and $\mathbf{X}_{IJ\times K}$ denote tall mode-1, mode-2 and mode-3 unfoldings, with $x_{i,j,k} = [\mathbf{X}_{JK\times I}]_{(k-1)J+j,i} = [\mathbf{X}_{KI\times J}]_{(i-1)K+k,j} = [\mathbf{X}_{IJ\times K}]_{(j-1)I+i,k}$. The *vec(.)* and *unvec(.)* operators are defined by

$$\mathbf{x}_{JKI} = \text{vec}(\mathbf{X}_{JK\times I}) \in \mathbb{C}^{JKI\times 1}$$
$$\leftrightarrow \mathbf{X}_{JK\times I} = \text{unvec}(\mathbf{x}_{JKI}).$$

1.2 PARAFAC and Nested PARAFAC decompositions

A PARAFAC decomposition [4,13] of a third-order tensor $\mathcal{X} \in \mathbb{C}^{I\times J\times K}$, with rank-$R$ and matrix factors $(\mathbf{A},\mathbf{B},\mathbf{C})$, will be noted $[\![\mathbf{A},\mathbf{B},\mathbf{C};R]\!]$. Tall and flat mode-1 matrix unfoldings of $\mathcal{X}$ are respectively given by

$$\mathbf{X}_{JK\times I} = (\mathbf{C} \diamond \mathbf{B})\mathbf{A}^T = (\mathbf{X}_{I\times JK})^T,$$

where $\diamond$ denotes the Khatri-Rao product. Similar mode-2 and mode-3 unfoldings can be obtained by permuting the factor matrices.

A 4^{th} Nested PARAFAC model [17,18] can be seen as a generalized model w.r.t.the PARAFAC. In this model a 4^{th}-order tensor can be reduced to two3^{rd}-order tensors that follows a PARAFAC model, by associating two of their original modes into a single one. The matrix factors related to the associated modes are

$$\mathcal{X} = [\![\mathbf{A},\mathbf{B},\mathbf{C};R_1]\!],$$
$$\mathcal{C} = [\![\mathbf{D},\mathbf{E},\mathbf{F};R_2]\!].$$

where $\mathbf{C}$ can be any matrix unfolding of $\mathcal{C}$.Note that $\mathbf{C}$ in (2) is any unfolded form of $\mathcal{C}$ represented in (3).

II. THREE-HOP SYSTEM

A one-way three-hop relay system is depicted in Fig. 1. The source (S) node wants to transmit its signal to the destination (D) node with the aid of unidirectional relays R_1 and R_2. The communication channels $\mathbf{H}^{(SR_1)} \in \mathbb{C}^{M_1\times M_S}$, $\mathbf{H}^{(R_1R_2)} \in \mathbb{C}^{M_2\times M_1}$ and $\mathbf{H}^{(R_2D)} \in \mathbb{C}^{M_D\times M_2}$ are considered to flat-fading and time-invariant during a transmission block

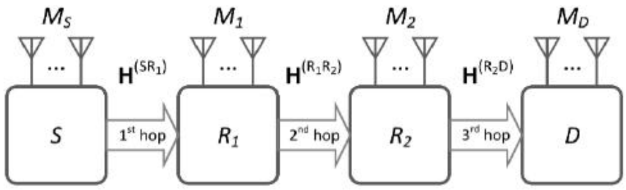

Fig.1: Three-hop one-way communication

Prior to the transmisstion, the source node applies a Khatri-Rao Space-Time (KRST) coding on its symbol matrix $\mathbf{S} \in \mathbb{C}^{N\times M_S}$ using the code matrix $\mathbf{C}^{P\times M_S}$. Just like in , N is the data-stream (number of symbol vectors) and P is the spreading source code length. Thus, in the first hop of Fig.1, the signals transmitted from S to R_1 become

$$\mathbf{W}^{(R_1)}_{M_1\times PN} = \mathbf{H}^{(SR_1)}(\mathbf{S} \diamond \mathbf{C})^T.$$

In the second hop, R_1 applies the Khatri-Rao ST coding over J, and R_1 transmits its signal to R_2. The signals arriving at this second relay are

$$\mathbf{W}^{(R_2)}_{M_2\times JPN} = \mathbf{H}^{(R_1R_2)}\left(\mathbf{W}^{(R_1)}_{PN\times M_1} \diamond \mathbf{G}^{(R_1)}\right)^T.$$

Equation (5) is intentionally written in the form of (4), such that there is a correspondence between the matrices that compose both signal models. For one, $\mathbf{G}^{(R_1)}$ has equivalent role of $\mathbf{C}$ on the R_1's side, while $\mathbf{W}^{(R_1)}_{PN\times M_1}$ and $\mathbf{S}$ represent the signals prior to the ST coding at the first relay and at source, respectively. The entris of $\mathbf{W}^{(R_2)}_{M_2\times JPN}$ could be stored in the 4^{th}-order tensor $\mathcal{W}^{(R_2)} \in \mathbb{C}^{M_2\times J\times P\times N}$ such as

$$w^{(R_2)}_{m_2,j,p,n} = \sum_{m_1=1}^{M_1} h^{(R_1R_2)}_{m_2,m_1} g^{(R_1)}_{j,m_1} \sum_{m_S=1}^{M_S} h^{(SR_1)}_{m_1,m_S} c^{(1)}_{p,m_S} s_{n,m_S}$$

that follows a Nested PARAFAC decomposition However, without needing to store the data, R_2 forwards the signals to the destination node (last hop of Fig. 1).

Before the forwarding process by R_2, this relay applies a new orthogonal KRST coding (similarly to (4) and (5)) with a code length K, such that after the transmission through $\mathbf{H}^{(R_2D)}$ we have

$$\mathbf{X}_{M_D\times KJPN} = \mathbf{H}^{(R_2D)}\left(\mathbf{W}^{(R_2)}_{JPN\times M_2} \diamond \mathbf{G}^{(R_2)}\right)^T. \qquad (2)$$

https://dx.doi.org/10.22161/ijaers.6.1.17 **ISSN: 2349-6495(P) | 2456-1908(O)**

Due to the third hop (third KRST coding), with the addition of the dimension of length K, the signals arriving at the destination node can be arranged in a 5^{th}-order tensor $\mathbf{X} \in \mathbb{C}^{M_D \times K \times J \times P \times N}$. Using (6), the scalar form of this tensor can be given by

$$x_{m_D,k,j,p,n} = \sum_{m_2=1}^{M_2} h_{m_D,m_2}^{(R_2D)} g_{k,m_2}^{(R_2)} w_{m_2,j,p,n}^{(R_2)}$$

$$= \sum_{m_2=1}^{M_2} h_{m_D,m_2}^{(R_2D)} g_{k,m_2}^{(R_2)} \times \sum_{m_1=1}^{M_1} h_{m_2,m_1}^{(R_1R_2)} g_{j,m_1}^{(R_1)} \times \sum_{m_S=1}^{M_S} h_{m_1,m_S}^{(SR_1)} c_{p,m_S} s_{n,m_S}.$$

Contrasting (8) with (6), the nesting nature of the Nested PARAFAC is kept at a higher-order due to the sequential KRST coding at each relay station. For the 4^{th} order model, the data can be processed directly from the 4^{th}-way tensor or through the two nested 3^{th}-order tensors, being the latter the best in terms of computational burden. Among different forms of processing the (received) 5^{th}-order tensor described (8), the data can be arranged to conform to three PARAFAC models, $\mathcal{X}^{(Z)}\mathbb{C}^{M_D KJ \times P \times N}$, $\mathcal{Z}^{(R_2)} \in \mathbb{C}^{M_D K \times J \times M_S}$ and $\mathcal{Z}^{(R_1)} \in \mathbb{C}^{M_D \times K \times M_1}$, i.e.

$$\mathcal{X}^{(Z)} = [\![\mathbf{Z}_{M_D KJ \times M_S}^{(R_2)}, \mathbf{C}, \mathbf{S}; M_S]\!],$$

$$\mathcal{Z}^{(R_2)} = \left[\!\left[\mathbf{Z}_{M_D K \times M_1}^{(R_1)}, \mathbf{G}^{(R_1)}, \left(\mathbf{H}^{(SR_1)}\right)^T; M_1 \right]\!\right],$$

$$\mathcal{Z}^{(R_1)} = \left[\!\left[\mathbf{H}^{(R_2D)}, \mathbf{G}^{(R_2)}, \left(\mathbf{H}^{(R_1R_2)}\right)^T; M_2 \right]\!\right],$$

where $\mathcal{X}^{(Z)}$ is obtained through the order reduction of $\mathcal{X}$ by associating its three first indices . The predilection for working with 3 these 3^{rd}-order tensors rather than directly with5^{th}-order tensorcomes from the fact that established tools and theorems dedicated to third-order PARAFAC models are well-established and could be more easily applied.

2.1 Noise terms

The additive noise terms on relays R_1 and R_2 can be respectively given by

$$\mathbf{V}_{M_2 \times JPN}^{(R_2)} = \mathbf{H}^{(R_1R_2)} \left(\mathbf{V}_{M_2 \times PN}^{(R_1)} \diamond \mathbf{G}^{(R_1)} \right)^T,$$

$$\mathbf{V}_{M_D \times KJPN}^{(R_D)} = \mathbf{H}^{(R_2D)} \left(\mathbf{V}_{M_2 \times JPN}^{(R_2)} \diamond \mathbf{G}^{(R_2)} \right)^T.$$

These forms follow the same unfolding order of (5) and (7). The matrices $\mathbf{V}_{M_2 \times PN}^{(R_1)}$, $\mathbf{V}_{M_2 \times JPN}^{(R_2)}$ and $\mathbf{V}_{M_D \times KJPN}^{(R_D)}$ are unfolded forms of the noise tensors $\mathrm{V}^{(R_1)} \in \mathbb{C}^{M_1 \times P \times N}$, $\mathrm{V}^{(R_2)} \in \mathbb{C}^{M_2 \times J \times P \times N}$and $\mathrm{V}^{(\mathrm{D})} \in \mathbb{C}^{M_D \times K \times J \times P \times N}$, that affect the inputs of R_1, R_2 and of the node D, respectively.

Note that $\mathrm{V}^{(R_2)}$ and $\mathbf{V}_{M_D \times KJPN}^{(R_D)}$ also follow Nested PARAFAC decompositions, and thus, its matrix factors, such as the channel and code matrices, might be uniquely identified. That is a interesting approach, as it would not require symbol transmission for the task of CSI retrieval.

III. TRIPLE KRF (TKRF) SEMI-BLIND RECEIVER

The objective of the semi-blind receiver installed at the destination is not only to decode the symbols transmitted by the source, but also to jointly estimate all channels of the 3-hop link. The use of the 4^{th}-order Nested PARAFAC decomposition employed by [?, 12] enabled the development of 3 semi-blind receivers in total, although others could have been presented for the same mdodel. Perhaps the most interesting (8) of those receivers is the one called DKRF, composed by two non-iterative, sequential Khatri-Rao Factorizations (KRF), which presented the same performance as the others, but with less computational complexity . The same idea can be extended from the two-hop systemto the three-hop one by adding up a third KRF factorization.

Let one write the mode-2 unfoldings of the tensors $\mathcal{X}^{(Z)}, \mathcal{Z}^{(R_2)}$ and $\mathcal{Z}^{(R_1)}$ respectively as

$$\mathbf{X}_{NM_D KJ \times P} = \left(\mathbf{Z}_{M_D KJ \times M_S}^{(R_2)} \diamond \mathbf{S} \right) \mathbf{C}^T,$$

$$\mathbf{Z}_{M_S M_D K \times J}^{(R_2)} = \left(\mathbf{Z}_{M_D K \times M_1}^{(R_1)} \diamond \left(\mathbf{H}^{(SR_1)}\right)^T \right) \left(\mathbf{G}^{(R_1)}\right)^T, \quad (13)$$

$$\mathbf{Z}_{M_1 M_D \times K}^{(R_1)} = \left(\mathbf{H}^{(R_2D)} \diamond \left(\mathbf{H}^{(R_1R_2)}\right)^T \right) \left(\mathbf{G}^{(R_2)}\right)^T. \quad (9)$$

The basic KRF factorization consists of reshaping each column of a Khatri-Rao product (10) into a matrix, and then approximating such rank-one (11) matrix as the outer product of two column vectors . The KRF algorithm is in Alg. 2

Here we admit the principle that the estimation of the symbols is indispensable, while the estimation of the channel is optional. This makes the TKRF receiver more flexible, since some of the steps for the estimation of individual channels can be neglected, resulting in the reduction of the global complexity and a relaxation of the identifiability conditions. The three (sequential) KRF of the TKRF receiver are called KRF-1, KRF-2 and KRF-3, and they basically differ in the inputs and outputs. The fluxogram of the TKRF receiver is shown in the Fig. 2, and the description of its inputs and outputs are given by:

- KRF-1: Symbol estimation (mandatory)
    - *Inputs*: $\mathbf{X}_{NM_D KJ \times P}$ and $\mathbf{C}$;
    - *Outputs*: $(\mathbf{Z}_{M_D KJ \times M_S}^{(R_2)}, \mathbf{S})$
- KRF-2 (optional)
    - *Inputs*: $(\mathbf{Z}_{M_S M_D K \times J}^{(R_2)}, \mathbf{G}^{(R_1)})$;
    - *Outputs*: $(\mathbf{Z}_{M_D K \times M_1}^{(R_1)}, \mathbf{H}^{(SR_1)})$
- KRF-3 (optional)
    - *Inputs*: $(\mathbf{Z}_{M_1 M_D \times K}^{(R_1)}, \mathbf{G}^{(R_2)})$;
    - *Outputs*: $(\mathbf{H}^{(R_2D)}, \mathbf{H}^{(R_1R_2)})$

https://dx.doi.org/10.22161/ijaers.6.1.17 **ISSN: 2349-6495(P) | 2456-1908(O)**

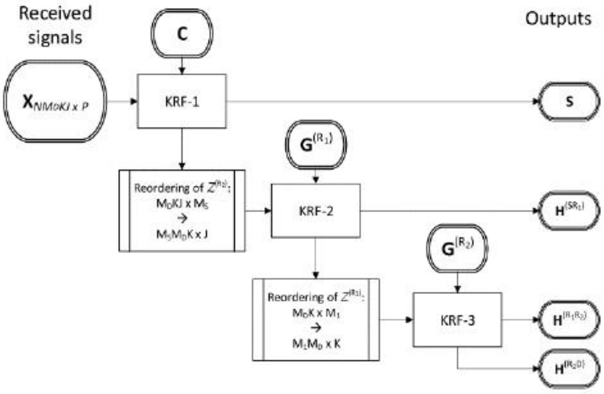

Fig.2: TKRF algorithm

3.1 Identifiability and Uniqueness Conditions

In this section, identifiability and uniqueness conditions are derived to the case where all matrices (symbols and channels) are to be estimated.

Theorem 1 (Identifibiality) *Let the source code matrix* $\boldsymbol{C}$ *and the relay code matrices* $\boldsymbol{G}^{(R_1)}$ *and* $\boldsymbol{G}^{(R_2)}$ *have full-rank. Necessary and sufficient identifiability condition to jointly estimate symbol* ($\boldsymbol{S}$) *and channel* ($\boldsymbol{H}^{(SR_1)}$, $\boldsymbol{H}^{(R_1R_2)}$ *and* $\boldsymbol{H}^{(R_2S)}$) *matrices are that*

$$P \geq M_S, \quad J \geq M_1 \text{ and } \quad K \geq M_2.$$

Proof. From the KRF algoritm (Alg. 2(c)@), the necessary (and only) condition to apply the column factorization is that $\mathbf{G}^T(\mathbf{G}^T)^{\dagger} = \mathbf{I}_R$. For the existence of the right inverse of $\mathbf{G}^T$, if $\mathbf{G}$ is full-rank, then it is necessary that $\mathbf{G}$ be also full column-rank. Once the TKRF receiver calls the KRF algorithm three times (i.e. KRF-1, KRF-2 and KRF-3), using one of three different correspondences at a time, i.e. $\mathbf{G} \Leftrightarrow \left(\mathbf{C}, \mathbf{G}^{(R_1)}, \mathbf{G}^{(R_2)}\right)$, then the necessary and sufficient identifiability condition, given that all code matrices are full-rank by Theorem 1, is simply (15).

Theorem 2 (Uniqueness) *Assume the following hypotheses: (a) the entries of the channel matrices are drawn from stochastic processes with continuous Gaussian distribution; (b) the identifiability hypotheses and conditions from Theorem 1 are met; (c) Symbol matrix is composed of random symbols, and the number of data-stream N is much greater than the number of source antennas* M_S. *Under such hypotheses, a sufficient but not necessary condition to ensure with very high probability the uniqueness solution at the output of the TRKF receiver is*

$$min(M_D, M_S, M_1, M_2) \geq |M_2 - M_1| + 2.$$

Proof. Model equations (10) and (11) belongs to a 4^{th}-order Nested PARAFAC decomposition of the data fully stored in $\mathcal{Z}^{(R_2)}$, so by using Theorem 2 from [12] with due correspondences, it is possible to ensure the essential uniqueness of matrix factors in (10) and (11) if the entries of $\mathbf{H}^{(R_1,R_2)}$ are drawn from a continous Gaussian distribution. Once this is the case, as stated by the hypotheses of Theorem 2 in this paper, then from [12] the uniqueness of the estimates of $\mathbf{H}^{(SR_1)}$, $\mathbf{H}^{(R_1R_2)}$ and $\mathbf{H}^{(R_2S)}$ are guaranteed if

$$k_{\mathbf{G}^{(R_1)}} + k_{(\mathbf{H}^{(SR_1)})^T} \geq \max(2M_1 - M_2, M_2) + 2,$$

$$k_{\mathbf{G}^{(R_2)}} + k_{\mathbf{H}^{(R_2D)}} \geq \max(2M_2 - M_1, M_1) + 2,$$

where $k_{\mathbf{A}}$ is the Kruskal rank of $\mathbf{A}$.

Once $\mathbf{G}^{(R_1)}$ and $\mathbf{G}^{(R_2)}$ are full column-rank to satisfy the identifiability condition of Theorem 1, then $k_{\mathbf{G}^{(R_1)}} = M_1$ and $k_{\mathbf{G}^{(R_2)}} = M_2$. Given the hypothesis on the channels, we have that $k_{(\mathbf{H}^{(SR_1)})^T} = \min(M_S, M_1)$ and $k_{\mathbf{H}^{(R_2D)}} = \min(M_D, M_2)$. Eqs. (17) and (18) respectively become

$$\min(M_S, M_1) \geq \max(M_1 - M_2, M_2 - M_1) + 2,$$

$$\min(M_D, M_2) \geq \max(M_2 - M_1, M_1 - M_2) + 2.$$

Finally, combining (19) and (20) leads to the condition (16).

Proven the uniqueness of the fourth-order model comprising the two three-order models (10) and (11), what is left is the need to find the uniqueness condition regarding (9). This third-order tensor model has the following Kruskal condition: (15)

$$k_{\mathbf{Z}^{(R_2)}_{M_DKJ \times M_S}} + k_{\mathbf{C}} + k_{\mathbf{S}} \geq 2M_S + 2.$$

From hypotheses (b) and (c) from Theorem 2, $\mathbf{C}$ and $\mathbf{S}$ (with very high probability) have full column-rank. Thus, $k_{\mathbf{C}} = M_S$ and $k_{\mathbf{S}} = M_S$, reducing (21) to $k_{\mathbf{Z}^{(R_2)}_{M_DKJ \times M_S}} \geq 2$. This is always true if $\mathbf{Z}^{(R_2)}_{M_DKJ \times M_S}$ does not have any zero column or any pair of linearly dependent columns . Since channel matrices are randomly drawn from Gaussian distributions, and $\mathbf{G}^{(R_1)}$ and $\mathbf{G}^{(R_2)}$ are full-rank, then this condition is satisfied with probability close to one.

3.2 Computational complexity

The KRF algorithm consists of multiples rank-one approximations using SVD. Apart from other eventual operations, such as buffering and memory allocation, one may count those SVD's as the cost-dominant process for each KRF routine. The cost of the algorithms in floating-point operations that compose the TKRF receiver are displayed in Table 1. Note that for a matrix of dimensions $I_1 \times I_2$, the complexity of its SVD computation is around O($I_1 I_2 min(I_1, I_2)$) [3].

(16)

Table.1: TKRF's Computational complexity in floating operations

	Condition	Complexity
KRF-1	$P \geq M_S$	$min(M_D KJ, N) M_D KJN M_S$
KRF-2	$J \geq M_1$	$min(M_D K, M_S) M_D K M_S M_1$
KRF-3	$K \geq M_2$	$min(M_D, M_1) M_D M_1 M_2$

https://dx.doi.org/10.22161/ijaers.6.1.17 ISSN: 2349-6495(P) | 2456-1908(O)

It is noteworthy that KRF-1 tends to be more complex than KRF-2, while the latter is likely more complex than KRF-3. One of the reasons is that there is likely reduction of the input data volume after each Khatri-Rao Factorization.

IV. PERFORMANCE EVALUATION

For the assessment of the functionality of the proposed receiver, Bit Error Rate (BER) and channel Normalized Mean Square Error (NMSE) are evaluated . The coding matrices $\mathbf{C}$, $\mathbf{G}^{(R_1)}$ and $\mathbf{G}^{(R_2)}$ are (truncated) DFT matrices, and we assume $\mathbf{H}^{(SR_1)} \sim \mathcal{CN}(0,1/M_S)$, $\mathbf{H}^{(R_1R_2)} \sim \mathcal{CN}(0,1/M_1)$ and $\mathbf{H}^{(R_2D)} \sim \mathcal{CN}(0,1/M_2)$. Symbol energy is given by E_S, and the additive noise samples at relays and destination nodes are complex standard normal random variables wih variance equal to one. The Bit Error Rate (BER) and Channel Normalized Mean Square Error (NMSE) curves are evaluated using 10^7 runs of Monte Carlo simulations.

The impact of the code length P and J, put in practice by the source and by the first relay station, has already been investigated in two-hop systems , so it is adequate to assume – and it was verified – that the KRST coding at R_2 also adds a new coding gain on the outcome of symbol estimation in function of K. Therefore, perhaps it is more interesting to evaluate how the TKRF receiver behaves when the size of cooperative network increases. In the proposed model, it means when M_S, M_1, M_2 and M_D increase. Fig. 3 demonstrates the BER curves for $M = M_S = M_1 = M_2 = M_D = \{2,3,4\}$. M_S is set to 2 to allow the same number of information symbols to be sent in all simulations. Coding spreading lengths obey the minimum values to satisfy identifiability condition in (15), and with $N = 50$, the uniqueness condition in Theorem 2 is also complied. For two modulations (4-PSK and 16-PSK), the TKRF receiver responded in a expected manner for a MIMO system: more antennas meant a greater diversity order and lower BER figures as E_S increase, while the higher the modulation order, the higher the BER value. According to Table 1, the estimation complexity from $M = 2$ to $M = 4$ increased almost 50 times. This huge increment came mostly from the KRF-1 routine, which corresponded to more than 98% of the overall complexity. Whilst this number does seem elevated, there is still a valuable energy gain to achieve a target BER (e.g. ≈ 10 dB at $\text{BER} = 10^{-4}$ for both 4-PSK and 8-PSK). Moreover, the decision to let the receiving node do all the work allows the use of the AF protocol at the relays, saving them from heavy power-consuming decoding processes. Finally, since channel estimation (KRF-2 and KRF-3 routines) offers very little complexity overall, a more frequent CSI feedback to the transmitting nodes would undoubtedly allow further power optimization.

The channel NMSE for the same set of simulation parameters is shown in Fig. 4, but only for the 4-PSK simulation. Besides, the curves for $M = 3$ is ommitted to facilitate the visualization.

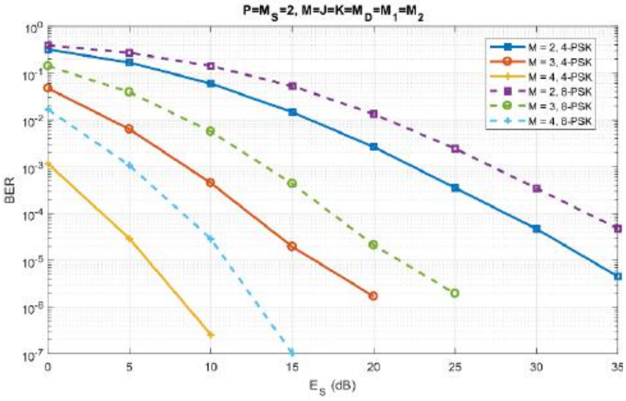

Fig.3: Bit Error Rate (BER)

The slopes of the curves indicate that CSI recovery responds differently for KRF-2 and KRF-3 in function of E_S – KRF-1 is responsible for symbol estimation. For $\mathbf{H}^{(SR_1)}$, approximately an order of magnitude of the error is reduce per decade, while for $\mathbf{H}^{(R_1R_2)}$ and $\mathbf{H}^{(R_2D)}$ the KRF-3 algorithm reduces the NMSE in two orders of magnitude per decade.

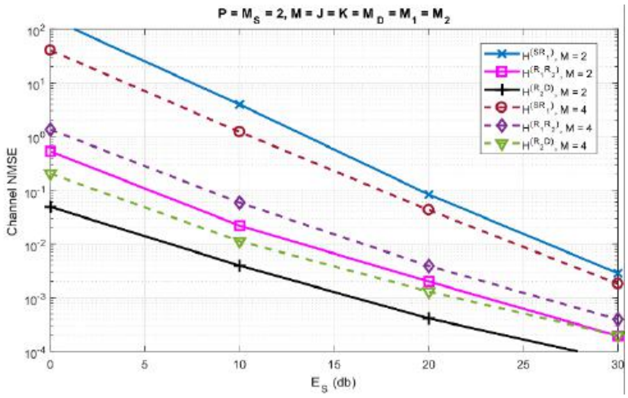

Fig.4: Channel NMSE

V. CONCLUSION

This article brought a solution for the issue of blind (symbol and channel) estimation in one-way, three-hop non regenerative relaying systems. Based on - the nesting concept of the 4^{th}-order Nested PARAFAC decomposition, this work extends this idea to 5^{th}-order tensors, allowing the leap from two-hop system to a three-hop system. Alongside the proposition of the new equations for this new derived tensor decomposition, this work brings an effective non-iterative semi-blind receiver. Computational simulations validate the proposed receiver and bring its performance in terms of symbol and channel estimation, as well as complexity and transmission rate.

It is important to regard the three-hop system (and its receiver) as an intermediate step between the two-hop system and a generalized multi-hop scenario. There is a clear pattern that indicates that several expressions presented in this paper (as the identifiability and uniqueness conditions) can be further generalized to any number of hops. However, there are few loose ends that need to be addressed in the next works: one is the complexity one, since greater number of hops also means a much larger volume of data; another one, now appreciated, is the expressive variety of possibilities that opens up to deal with the data and to solve the issue of joint symbol and channel estimation in a multi-hop scenario.

ACKNOWLEDGEMENTS

This work has been supported by FAPESP-Brazil, under project 2016/26032-4.

REFERENCES

[1] M. Biguesh and A.B. Gershman. Training-based MIMO channel estimation: a study of estimator tradeoffs and optimal training signals. *IEEE Transactions on Signal Processing*, 54(3):884–893, 2006.

[2] Í. V. Cavalcante, A. L. F. de Almeida, and M. Haardt. Tensor-based approach to channel estimation in amplify-and-forward MIMO relaying systems. In *Proceedings in IEEE Sensor Array and Multichannel Signal Processing Woskshop (SAM2014)*, pages 1–4, La Coruña , Spain, 2014.

[3] Gene H. Golub and Charles F. Van Loan. *Matrix Computations*. Johns Hopkins University Press, Baltimore, MD, USA, 1996.

[4] R. A. Harshman. Foundations of the PARAFAC procedure: Models and conditions for an "explanatory" multimodal factor analysis. *UCLA Working Papers in Phonetics*, 16:1–84, Dec. 1970.

[5] P. Lioliou and M. Viberg. Least-squares based channel estimation for MIMO relays. In *International ITG Workshop on Smart Antennas, 2008. WSA 2008*, pages 90–95, Feb 2008.

[6] Florian Roemer and Martin Haardt. Tensor-based channel estimation (TENCE) for two-way relaying with multiple antennas and spatial reuse. In *IEEE International Conference on Acoustics, Speech and Signal Processing (ICASSP)*, pages 3641–3644, Taipei, Taiwan, April 2009.

[7] Yue Rong, M.R.A. Khandaker, and Yong Xiang. Channel estimation of dual-hop MIMO relay system via parallel factor analysis. *IEEE Transactions on Wireless Communications*, 11(6):2224 –2233, Jun. 2012.

[8] Yue Rong, Xiaojun Tang, and Yingbo Hua. A unified framework for optimizing linear nonregenerative multicarrier MIMO relay communication systems. *IEEE Transactions on Signal Processing*, 57(12):4837–4851, Dec. 2009.

[9] Yue Rong. Optimal joint source and relay beamforming for MIMO relays with direct link. *IEEE Communications Letters*, 14(5):390–392, May 2010.

[10] M.H. Shariat, M. Biguesh, and S. Gazor. Relay design for SNR maximization in MIMO communication systems. In *5th International Symposium on Telecommunications (IST)*, pages 313–317, Tehran, Iran, 2010.

[11] L. R. Ximenes, G. Favier, A. L. F. de Almeida, and Y. C. B. Silva. PARAFAC-PARATUCK semi-blind receivers for two-hop cooperative MIMO relay systems. *IEEE Transactions on Signal Processing*, 62(14):3604–3615, July 2014.

[12] L. R. Ximenes, G. Favier, and A. L. F. de Almeida, "Semi-blind receivers for non-regenerative cooperative MIMO communications based on nested PARAFAC modeling," *IEEE Trans. Signal Process.*, vol. 63, no. 18, pp. 4985–4998, August 2015.

[13] N. D. Sidiropoulos, L. De Lathauwer, X. Fu, K. Huang, E. E. Papalexakis, and C. Faloutsos, "Tensor Decomposition for Signal Processing and Machine Learning," *IEEE Trans. Signal Process.*, vol. 65, no. 13, pp. 3551-3582, July 2017.

[14] L. R. Ximenes, G. Favier, and A. L. F. de Almeida,"Closed-Form Semi-Blind Receiver For MIMO Relay Systems Using Double Khatri-Rao Space-Time Coding,"*IEEE Signal Process. Lett.*, vol. 24, no. 3, pp. 316-320, Mar. 2016

[15] K. Liu, A. Sadek, W. Su, and A. Kwasinski, *Cooperative communications and networking*. 1em plus 0.5em minus 0.4em Boston, MA, USA: Cambridge University Press, 2008.

[16] H. Kaur, M. Khosla and R. K. Sarin, "Channel estimation in a MIMO relay system: Challenges and approaches channel estimation in MIMO relay system: A review," *2018 2nd International Conference on Inventive Systems and Control (ICISC)*, Coimbatore, 2018, pp. 203-214.

[17] A. L. F. de Almeida and G. Favier, "Double Khatri-Rao space-time-frequency coding using semi-blind PARAFAC based receiver," *IEEE Signal Process. Lett.*, vol. 20, no. 5, pp. 471–474, 2013.

[18] W. de C. Freitas, G. Favier, and A. L. F. de Almeida, "Sequential Closed-Form Semiblind Receiver for Space-Time Coded Multihop Relaying Systems," *IEEE Signal Process. Lett.*, vol. 24, no. 12, pp. 1773-1777, Dec. 2017